Sieve Tube Unloading and Post-Phloem Transport of Fluorescent Tracers and Proteins Injected into Sieve Tubes via Severed Aphid Stylets[1]

Donald B. Fisher* and Cora E. Cash-Clark[2]

Department of Botany, Washington State University, Pullman, Washington 99164–4238

A variety of fluorescent tracers and proteins were injected via severed aphid stylets into the sieve tubes of wheat (*Triticum aestivum* L.) grains to evaluate the dimensions of plasmodesmal channels involved in sieve element/companion cell (SE/CC) unloading and post-phloem transport. In the post-phloem pathway, where diffusion is the predominant mode of transport, the largest molecule to show mobility was 16-kD dextran, with a Stokes radius of 2.6 nm. This suggests that the aqueous channels for cell-to-cell transport must be about 8 nm in diameter. Even the largest tracer injected into the sieve tubes, 400-kD fluorescein-labeled Ficoll with a Stokes radius of about 11 nm, was unloaded from the SE/CC complex. However, in contrast to smaller tracers (≤3 kD, with a Stokes radius ≤ 1.2 nm), the unloading of fluorescein-labeled Ficoll and other large molecules from the SE/CC complex showed an irregular, patchy distribution, with no further movement along the post-phloem pathway. Either the plasmodesmal channels involved in SE/CC unloading are exceptionally large (perhaps as much as 42 nm in diameter), with only a very small fraction of plasmodesmata being conductive, or the larger tracers damage the plasmodesmata in some way, enlarging smaller channels.

In most sinks, assimilates follow a symplastic pathway as they move out of the sieve element/companion cell (SE/CC) complex and along the immediate post-phloem pathway (Fisher and Oparka, 1996; Patrick, 1997). Given the high assimilate fluxes at these steps, the dimensions of the aqueous cell-to-cell channels involved are important in the ability of plasmodesmata to accommodate such rapid movement. In two instances, corn root tips (Bret-Hart and Silk, 1994) and wheat grains (Wang and Fisher, 1994b), available estimates of symplastic conductance appeared to be too low to support the observed rates of post-phloem movement, assuming the frequently observed mass exclusion limit for plasmodesmata of about 800 D. In addition to the resistance of the post-phloem pathway, a high transport resistance is indicated for the SE/CC unloading step by the typically large differential in concentration and pressure between sieve tubes and adjacent sink cells. This differential is about 1.0 MPa in wheat grains (Fisher, 1995; Fisher and Cash-Clark, 2000) and 0.7 MPa in barley roots (Pritchard, 1996).

The dimensions of cell-to-cell transport channels in sinks are also important in the context of macromolecule movement. While their concentration is low, a large number of proteins of up to 200 kD are present in sieve tube exudate (Fisher et al., 1992; Nakamura et al., 1993). Presumably, they exit the sieve tubes on reaching a sink, and perhaps move along the post-phloem pathway. Potentially, some phloem-mobile proteins may be involved in source-to-sink signaling (Mezitt and Lucas, 1996). Although no such function has been established to date, cell-to-cell movement of several locally synthesized morphogenetic proteins has been observed or strongly inferred to occur in shoot meristems (Ding, 1998).

Several observations indicate that plasmodesmata involved in SE/CC unloading and post-phloem transport can accommodate the movement of molecules substantially larger than the 800-D mass exclusion limit characteristic of most plasmodesmata. Dextrans of at least 10 kD are mobile in the maternal post-phloem pathway of wheat grains (Wang and Fisher, 1994b). Green fluorescent protein (GFP) (27 kD) expressed in the companion cells of Arabidopsis (Imlau et al., 1999) or tobacco (Oparka et al., 1999) source leaves was unloaded from sieve tubes and moved extensively along the post-phloem pathway in a diversity of sinks including young leaves, root tips, and ovules. These observations indicate that plasmodesmata involved in assimilate import are modified to accommodate high-assimilate fluxes. They may also accommodate non-specific movement of smaller proteins.

Intercellular protein trafficking has been shown in a number of cases to involve specific interaction between the protein and plasmodesmata, although such interaction does not appear to be universal. Viral movement proteins, such as STEP (Sieve Tube Exudate Protein) and KNOTTED1, all capable of trafficking from cell to cell, also up-regulate the plasmodesmal mass exclusion limit to 10 to 40 kD for dextrans in mesophyll cells (for review, see Mezitt

[1] This work was supported by the National Science Foundation (grant no. IBN–9514188).

[2] Present e-mail address: tclark2@iusb.edu.

* Corresponding author; e-mail dbfisher@wsu.edu.

and Lucas, 1996). Up-regulation was observed for STEPs as small as 10 to 20 kD. Experiments with mutant proteins defective in movement provide evidence for the required specific interaction between the mobile protein and plasmodesmata (Mezitt and Lucas, 1996). For GFP, however, such specific interaction is unlikely. Similarly, phloem-specific expression of the snowdrop (*Galanthus nivalis*) lectin in tobacco resulted in the movement of the lectin into sieve tubes, as indicated by its appearance in aphid honeydew (Shi et al., 1994). Here, too, the involvement of a recognition factor in movement from companion cells into the sieve tubes is improbable.

To investigate the dimensions of the plasmodesmal channels involved in sieve tube unloading and post-phloem transport in wheat grains, a wide range of fluorescent tracers and several proteins were pressure-injected into sieve tubes via severed aphid stylets. The experimental approach was suggested by procedures used for the manometric measurement of turgor pressure in sieve tubes (Wright and Fisher, 1980; Fisher and Cash-Clark, 2000).

RESULTS

Success Rate

Not surprisingly, the proportion of successful injections was inversely related to sieve tube turgor. About a third of attempts with detached grains (turgor approximately 0.1–0.3 MPa) resulted in moderate to strong tracer levels in the crease tissues. Injections into the phloem of attached grains (turgor approximately 1 MPa) had about a 20% success rate, while injections into the rachilla phloem (turgor $>$ 2 MPa) resulted in the movement of fluorescence into the grain in only about 5% to 10% of attempts. These percentages were lower than expected, since turgor measurements had a high success rate at all sites (Fisher and Cash-Clark, 2000). To ensure that the stylets and phloem in those experiments remained conductive after exudate movement stopped, we clipped off the tips of the manometers, whereupon exudation almost invariably resumed. While leaks often occurred even during successful injections, reversal of flow often elicited a sealing response by the sieve tube. Exogenous solutes did not appear to be a consistent factor in the sealing response, which could occur even after a manometric pressure measurement (Fisher and Cash-Clark, 2000), when heat was applied to the compressed air pocket. In this case, no exogenous solutes were present, and the exudate being injected had flowed from the sieve tube just moments before.

Several factors made it impossible to control the rate or amount of injection. Because of the high frequency of leaks (usually not detectable until the end of the injection period) and sealing of the sieve tube after unknown intervals (stylets usually were not exuding at the end of the injection period), the amount of tracer injected varied substantially. The observations reported are confined to those in which the level of fluorescence was distinct and clearly above endogenous fluorescence levels.

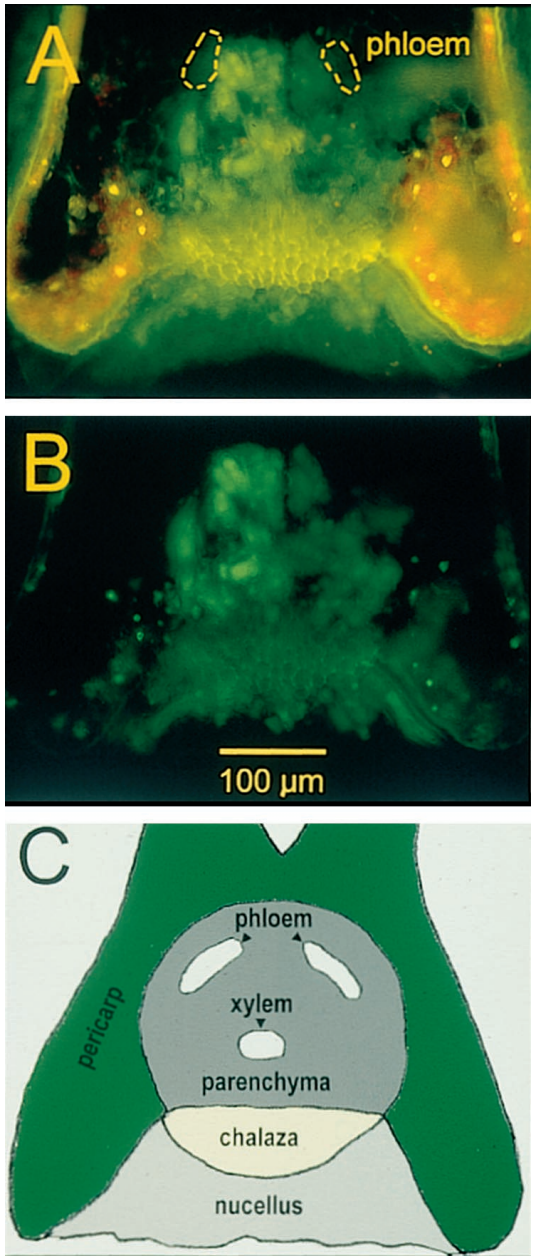

Figure 1. Hand-cut fresh cross-section showing the distribution of 3-kD F-dextran (R_s = approximately 1.2 nm) in the crease tissues after injection into a sieve tube in an attached grain. Injection took place over a 1-h period, after which the grain was sectioned. A, Fluorescence micrograph taken with a long-pass barrier filter to show autofluorescence, allowing better visualization of the tissues. Red and yellow are, respectively, chlorophyll autofluorescence in the pericarp and wall deposits in the chalaza and testa; green is F-dextran. B, Same section as A, but taken with a band-pass barrier filter to eliminate most of the autofluorescence at longer wavelengths. C, Diagram showing the tissues in the crease region of a wheat grain.

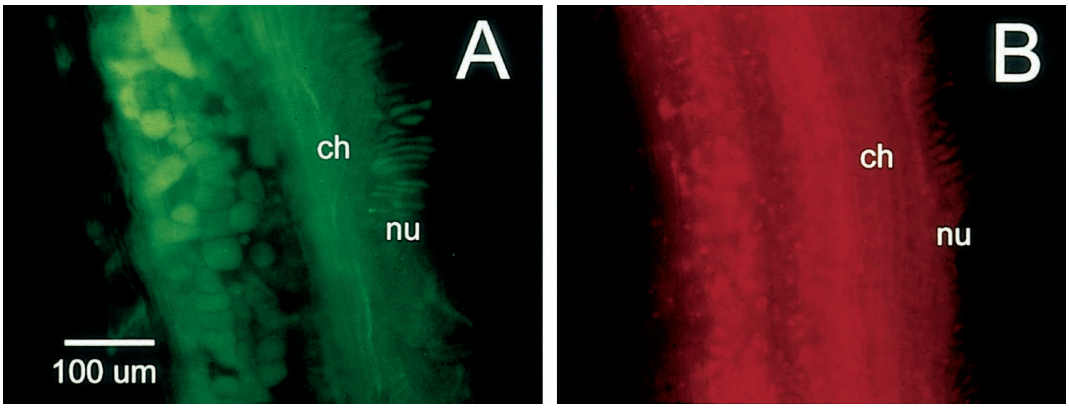

Figure 2. Fluorescence micrographs of hand-cut longitudinal fresh sections through the crease tissues after 2-h injections of 3-kD dextrans (R_s = approximately 1.2 nm). A, Distribution of 3-kD F-dextran. Unloading is fairly even along the phloem, and F-dextran has moved into the nucellus (nu). Except for some autofluorescence in the chalaza (ch), F-dextran accounts for virtually all of the fluorescence. B, Distribution of 3-kD R-dextran. Intercellular mobility is similar to that of 3-kD F-dextran; however, in contrast to the uniform within-cell fluorescence of 3-kD F-dextran, R-dextran is localized in globules, suggesting that it has been sequestered into a subcellular compartment, presumably the vacuole.

The largest tracers (≥70 kD) sometimes accumulated in the sieve tube on either side of the injection site, apparently reducing further movement or blocking it altogether. This was most pronounced for injections into the rachilla. Attempts to inject 44-nm (diameter) fluorescent microspheres (Molecular Probes) were unsuccessful, perhaps due to aggregation. The spheres moved at most only a few sieve elements from the injection site, stopping abruptly at a sieve plate with no unloading from the SE/CC complex.

Repeated attempts to inject tracers into stylets on barley root tips were unsuccessful.

Low-Molecular-Mass Compounds (<3 kD)

In most successful injections, low-molecular-mass tracers unloaded fairly evenly along the length of the vascular bundle (Figs. 1–3). By the end of the injection period (40–80 min), fluorescence was usually distributed throughout the vascular parenchyma and had moved across the chalaza into the nucellus. While 3-kD F-dextran (R_s = approximately 1.2 nm) showed a fairly uniform subcellular distribution (Figs. 1 and 2A; also see Wang and Fisher, 1994b), low-molecular-mass fluorochromes including F-stachyose (not shown), 3-kD R-dextran (Fig. 2B), and carboxyfluorescein (Fig. 3) showed a distinctly globular pattern, indicating that these tracers had been sequestered into vacuoles. That an effective process for xenobiotic sequestration occurs in these tissues was shown by incubating fresh sections in 0.1 mM BmCl in perfusion medium. This resulted in the rapid appearance of a strongly fluorescent product, presumably the conjugate of BmCl with glutathione (Coleman et al., 1997) into vacuoles (Fig. 4).

In some injections of 3-kD F-dextran, unloading "hot spots" were present, in which single cells bordering the phloem were intensely fluorescent in comparison with their neighbors (not illustrated for 3-kD F-dextran; see the next section). When only small amounts of fluorochrome were injected, very little movement along the post-phloem pathway occurred, perhaps due to more efficient sequestering of the smaller amount of fluorochrome.

Higher-Molecular-Mass Dextrans and Ficoll

Surprisingly, even the largest fluorochrome successfully injected, 400-kD F-Ficoll (R_s = approximately 11 nm; extrapolated from Laurent and Granath [1967]), was unloaded from the SE/CC complex. However, unloading occurred mostly at single-cell "hot spots" along the phloem (Fig. 5A), with no subsequent movement along the post-phloem pathway. Often, but by no means always (e.g. Fig. 5A), unloading occurred primarily in the distal third of the grain. The larger F-dextrans (70 kD, R_s = approximately 5.9 nm, Fig. 5B; and 40 kD, R_s = approxi-

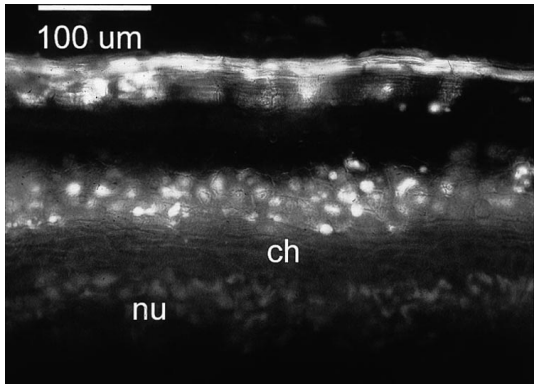

Figure 3. Distribution of carboxyfluorescein (R_s = 0.6 nm) after a 2-h injection. Intercellular mobility is similar to that for the 3-kD dextrans (Fig. 2). As for R-dextran, the subcellular distribution has a globular appearance, suggesting sequestration into vacuoles. ch, Chalaza; nu, nucellus.

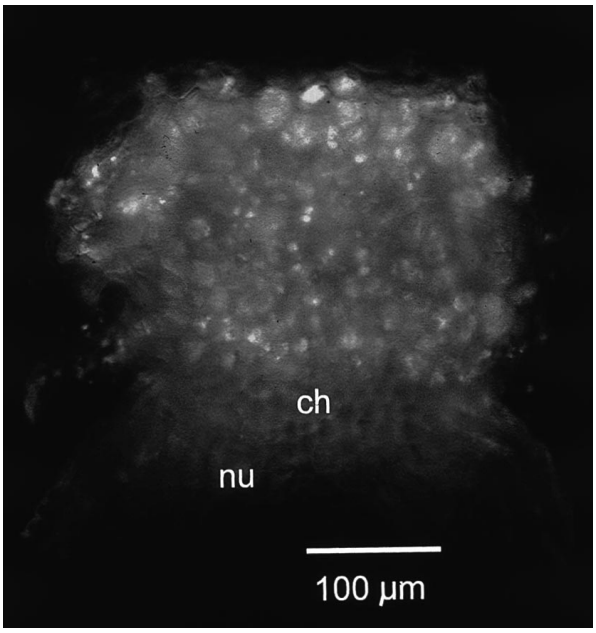

Figure 4. Distribution of a strongly fluorescent product, presumably the glutathione conjugate of monochlorobimane (Coleman et al., 1997), after incubating fresh sections with monochlorobimane in perfusion medium for 30 min, followed by a 40-min wash. ch, Chalaza; nu, nucellus.

mately 4.3 nm, Fig. 6A) showed a pattern of movement (patchy unloading with no post-phloem movement) similar to that of 400-kD F-Ficoll. Even when 20 h elapsed between injection and sectioning, 40-kD (Fig. 6B) and 20-kD dextrans showed little or no post-phloem movement.

By comparison, 10-kD (R_s = approximately 2.0 nm) and 16-kD (R_s = approximately 2.6 nm) F-dextran tended to unload more uniformly along the phloem, although with more "hot spots" than for 3-kD dextrans. Soon after injection, only slight post-phloem movement was evident (Fig. 7A). After 24 h, however, both dextrans showed substantial movement into the nucellus (Fig. 7, B and C).

Larger dextrans and Ficoll were excluded from the nucleus (not shown); surprisingly, even 3-kD F-dextran was excluded from the nucleus (Fig. 8). After 5 min in a boiling water bath, 10-kD and larger dextrans were retained within cells for many hours (Fig. 9); only 3-kD dextran was lost slowly after heating. Thus, there was no indication that any of these tracers might have been degraded from its nominal size.

Proteins

Fluorescein-labeled lactalbumin (14.8 kD; R_s = 2.0 nm by interpolation; Johnson et al., 1996) was the smallest protein injected. Some unloading occurred at infrequent "hot spots" (not shown), with no evident post-phloem movement in grains sectioned immediately after injection. (No observations were made in which sectioning was delayed.) GFP (27 kD; R_s uncertain but perhaps approximately 1.8 nm; see "Discussion") was unloaded more extensively, although unloading was still uneven (Fig. 10A), with no immediate post-phloem movement. Several hours after injection, GFP often had moved throughout much of the vascular parenchyma, but was not observed to move to the nucellus (Fig. 10B).

Injection of GUS (monomer = 68 kD; R_s = approximately 3.3 nm) resulted in scattered unloading along the phloem (Fig. 11A), with no evident post-phloem movement even when sectioning was delayed for 4 h after injection.

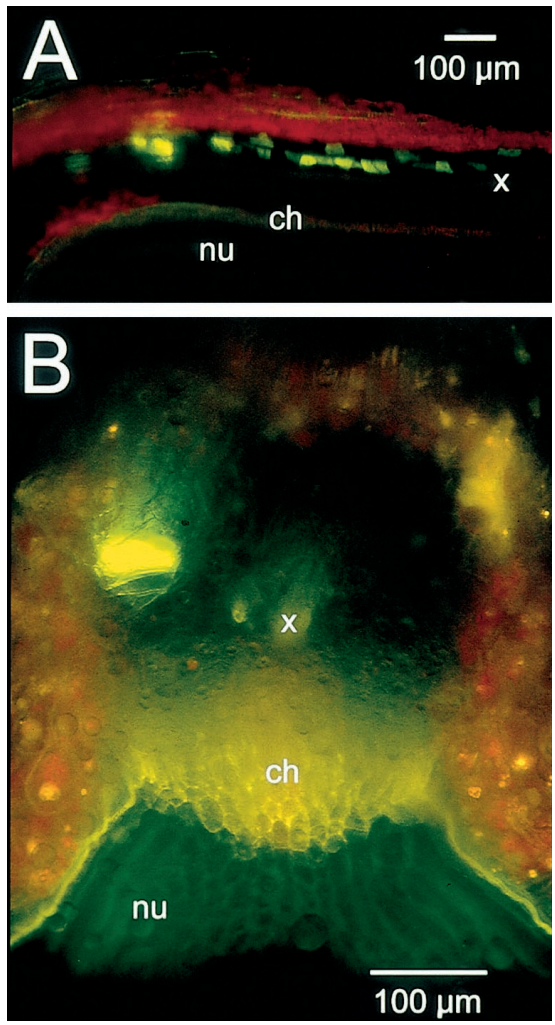

Figure 5. Distribution of the largest fluorescent tracers injected, 400-kD F-Ficoll and 70-kD F-dextran (R_s = approximately 11 and 5.9 nm, respectively), showing the characteristic patchiness of phloem unloading and the absence of subsequent post-phloem movement. The pictures were taken with a long-pass barrier filter to include autofluorescence. Red is chlorophyll. A, Longitudinal section, showing "hot spots" of 400-kD F-Ficoll unloading (yellow-green fluorescence) into scattered cells along the sieve tubes. F-Ficoll was injected for 1 h into an attached grain. B, Distribution of 70-kD F-dextran in a cross-section after a 2-h injection into an attached grain. Cell wall-associated autofluorescence occurs in the chalaza (yellow) and the nucellus (yellow-green). ch, Chalaza; nu, nucellus; x, xylem.

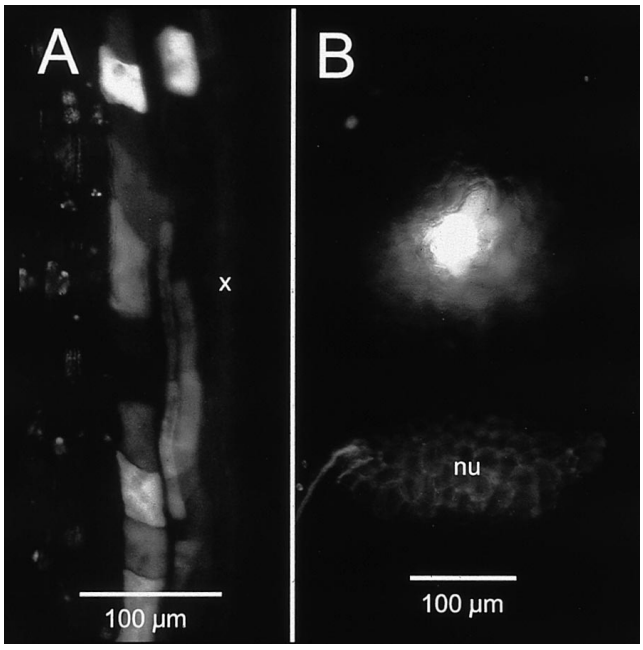

Figure 6. Distribution of 40-kD F-dextran (R_s = approximately 4.3 nm) after injection into attached grains. A, Longitudinal section taken immediately after a 1-h injection. x, Xylem. B, Cross-section taken 20 h after injection. There is slight, if any, movement away from cells immediately surrounding the phloem. nu, Nucellus.

Co-Injection Experiments

Because of the dissimilarity in unloading patterns for large versus small molecules, several tracer pairs were co-injected to determine the extent to which large and small molecules might interact. When GUS and 3-kD F-dextran were co-injected, unloading of GUS from the phloem was scattered (not shown), as was observed with GUS alone (Fig. 11A). Distribution of the much smaller dextran, found earlier to unload fairly uniformly and to move freely along the post-phloem pathway (Figs. 1 and 2), was now largely, but not entirely, coincident with GUS (Fig. 11, B and C). Somewhat similar results were obtained when F-Ficoll and 3-kD R-dextran were co-injected, although both were retained almost entirely within the sieve tubes, with virtually no unloading (not shown).

Movement through the Grain Pedicel

Although injections into the rachilla had a low success rate (only a single injection of F-Ficoll was successful), all of the F-dextrans (from 3 to 70 Kd) and F-Ficoll (400 kD) moved into the grain. Characteristics of sieve tube unloading (i.e. the patchiness of unloading) and the extent of subsequent post-phloem movement were consistent with those described above for injections into grain sieve tubes. Considerable spreading of the fluorochromes from the injected vein occurred in the anastomosing vascular bundles immediately below the point of grain insertion (Fig. 12A). In one instance, 3-kD F-dextran was detected as it bypassed the xylem discontinuity in the pedicel, revealing the ring of sieve tubes surrounding the central core of modified, non-conducting xylem tracheary elements (Fig. 12B). As a result of this spreading, unloading occurred from more sieve tubes in rachilla-injected grains (Fig. 12C).

Detached Grains

Because transport patterns in attached grains are more relevant to normal grain physiology, fewer injections were made into detached grains. However, almost the entire range of injections was also carried out with detached grains, with generally similar results. These include the patchiness of unloading with F-Ficoll and the larger dextrans and the relative mobilities of the tracers in post-phloem movement. However, the movement of 3-kD dextrans seemed

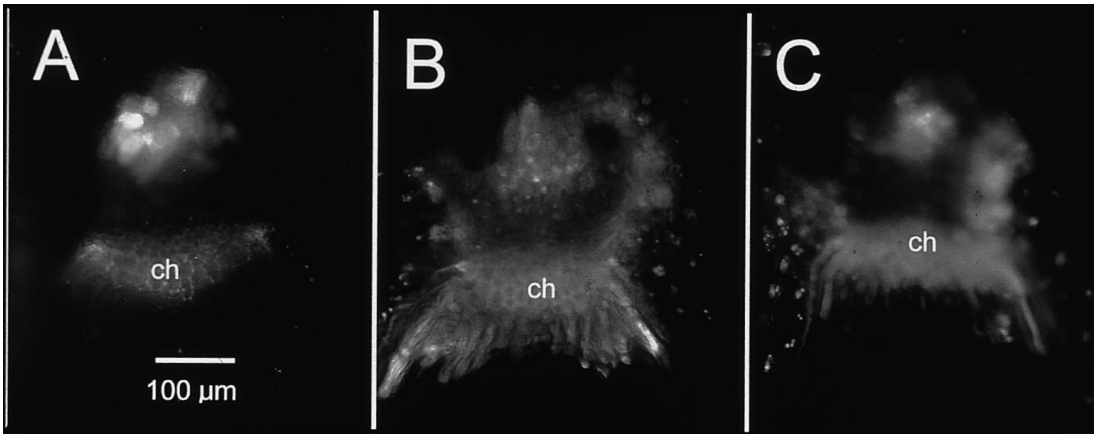

Figure 7. Distribution of 10- and 16-kD F-dextrans (R_s = approximately 2.0 and 2.6 nm, respectively) after injection into attached grains. On sectioning 40 min after a 40-min injection period, there appeared to be only weak movement of 10-kD dextran into the nucellus (A). One day after injection, strong movement of 10-kD F-dextran (B) and 16-kD F-dextran (C) had occurred into the nucellus. ch, Chalaza.

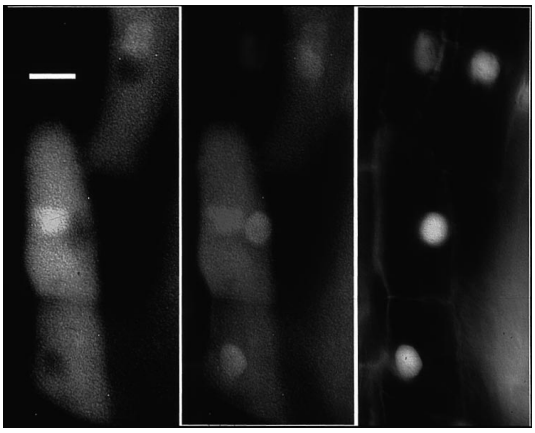

Figure 8. All F-dextrans, even the 3-kD F-dextran shown here, were excluded from the nucleus, demonstrating that the conjugates remained intact. Left, F-dextran distribution (bar = 20 μm). Center, Superimposed images. Right, Nuclei stained with Hoechst stain.

somewhat slower (little fluorescence was present in the nucellus immediately after injection), and 24 h after injection, 10- and 16-kD F-dextrans had diffused throughout the vascular parenchyma but only traces occasionally reached the nucellus (similar to the distribution shown for GFP in Fig. 10B; compare with Fig. 7, B and C).

DISCUSSION

Molecular Sizes

There is no unique relationship between molecular mass and molecular dimensions, especially when comparing different classes of molecules such as dextrans and proteins. A 20-kD dextran, for example, has the same Stokes radius (3.0 nm) as a 51-kD globular protein. For this reason, the practice of referring to "size" in terms of molecular mass will be avoided. Instead, because molecular dimensions are central to the following discussion, "size" will be given as the Stokes radius. However, as the dimension of an equivalent sphere having the same hydrodynamic drag during unhindered diffusion as the molecule in question, it too has distinct limitations as a measure of molecular size. This is especially true for interactions between a pore and flexible, asymmetric, and/or highly charged molecules. In a biological context, these issues have been dealt with most thoroughly in glomerular filtration (for review, see Maddox et al., 1992), which involves the pressure-driven flow of solution through channels about 0.2 μm long and 10 nm in diameter, roughly comparable to the dimensions of aqueous channels in plasmodesmata. However, at 0.003 MPa, the pressure differential is far less than for SE/CC unloading.

Assumed relationships between molecular mass and Stokes radii are interpolated from the relationships given by Jorgensen and Moller (1979) for dextrans and by le Maire et al. (1986) for globular proteins. For reasons that are unclear, the latter approach

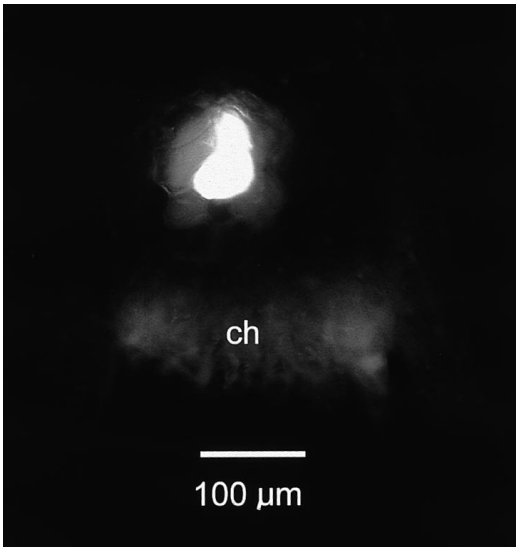

Figure 9. F-dextrans larger than 3 kD were retained in cells long after they had been killed by immersion in water at 100°C. Here, 10-kD F-dextran is shown 3 h after a 5-min treatment at 100°C. ch, Chalaza.

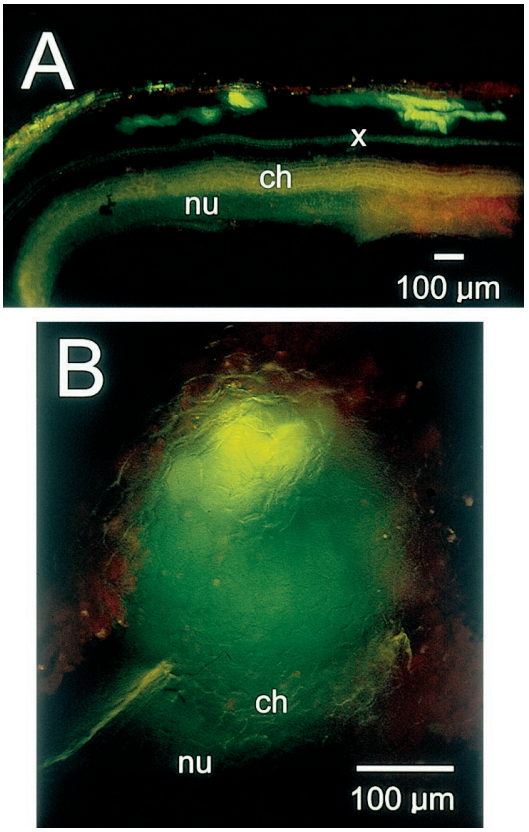

Figure 10. Distribution of GFP (R_s uncertain, perhaps 1.8 nm; see text) after injection into attached grains. A, Longitudinal section taken immediately after injection, showing patchy unloading along the phloem. B, Cross-section taken 4 h after injection, showing movement up to, but not beyond, the chalaza. ch, Chalaza; nu, nucellus; x, xylem.

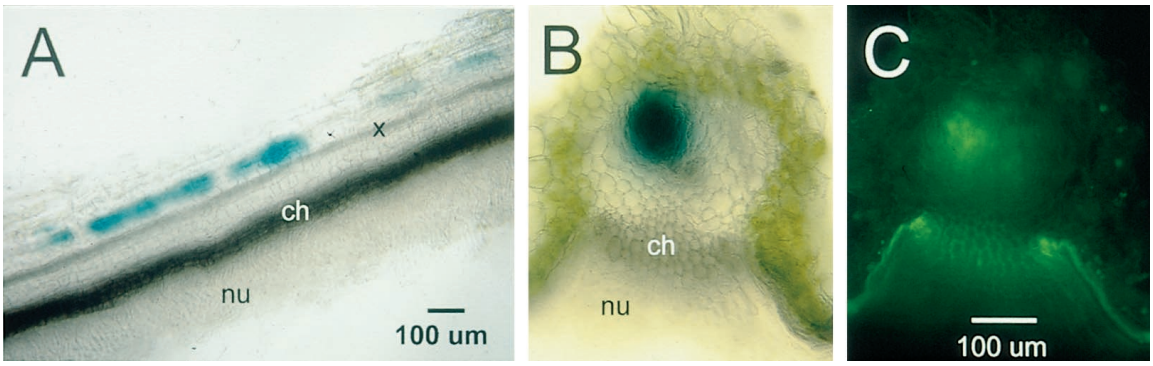

Figure 11. Distribution of GUS (monomeric R_s = approximately 3.3 nm) when injected alone (A) or co-injected with 3-kD F-dextran (B). In both experiments, GUS showed patchy unloading with no evidence of subsequent post-phloem movement. The distribution of co-injected 3-kD F-dextran (C) was almost entirely coincident with that of GUS (B). (The chalazal walls show some autofluorescence.) The section shown in A was partially cleared with 80% (v/v) ethanol. ch, Chalaza; nu, nucellus; x, xylem.

gives a much larger value for GFP (2.4 nm) than would be expected from crystallographic measurements (Ormo et al., 1996; Yang et al., 1996), which show a barrel-like structure 2.4 to 3.0 nm in diameter and 4 nm long. Since the latter are experimentally determined dimensions, the R_s for GFP will be approximated as 1.8 nm. However, it should be noted that the mobility of GFP was more comparable to 2.6-nm dextran than to smaller dextrans.

Post-Phloem Pathway

In general, our observations provide confirmatory support for the concept that plasmodesmata along the post-phloem pathway are specialized for their transport function by having a relatively high permeability. The results increase somewhat our previous estimate of dextran mobility in this tissue (Wang and Fisher, 1994b), in which we judged the dextran with an R_s of 2.4 nm (approximately 14 kD) to be immobile. However, those experiments involved a much shorter transport time (30 min) compared with our present observations, in which 2.6-nm dextran (approximately 16 kD) did not move perceptibly in 1 h, but showed clear movement after a 12-h transport period (Fig. 7).

With some caveats, plasmodesmal permeability along the post-phloem pathway in wheat grains appears quite similar to that found by Oparka et al. (1999) for tobacco sink leaves. By fusing GFP with various-sized proteins, they estimated an upper limit for mobility of somewhat over 50 kD (interpolated R_s approximately 3.0 nm).

Since 20-kD dextran (R_s also approximately 3.0 nm) appeared to be immobile in wheat grains, plasmodesmal permeability there may be somewhat lower than for tobacco sink leaves. This is also suggested by the failure of GFP to move into the nucellus (Fig. 10B). However, as for GFP itself, our interpolation may overestimate the actual dimensions of the GFP fusion proteins. Also, Oparka et al.'s (1999) experiments based on plasmid bombardment involved a longer transport period and ongoing synthesis of the GFP fusion protein, in contrast to the pulse of injected tracer in our experiments. Finally, ambiguities arise in comparing such different tracers as proteins and dextrans. For a given R_s, dextrans occupy a larger volume than a protein because of their somewhat loose, randomly coiled conformation, making them (theoretically, at least) less mobile in small pores than a compact, rigid protein of the same R_s (Davidson and Deen, 1988a).

Experimentally, however, anomalously high dextran mobility has been observed in homoporous polycarbonate membranes (Bohrer et al., 1984) and in glomerular filtration (Rennke and Venkatachalam, 1979). While this relatively greater mobility has been ascribed to movement by "reptation," or end-on movement of the molecule along the pore axis, this is not supported by Davidson and Deen's (1988a, 1988b) theoretical analysis of flexible polymer movement in small pores. Since their analysis is consistent with observations on other flexible polymers, the results with dextran are viewed as anomalous. They suggest that unrecognized attractive interactions between dextran and the pore wall may facilitate dextran movement at higher-than-predicted rates. Thus, perhaps the main reservation in comparing our observations with those of Oparka et al. (1999) concerns possible deviations from theoretically expected properties of hindered diffusion by both proteins and dextrans. However, this reservation is no greater than comparisons between dextran and protein movement in other investigations of symplastic transport.

Subject to the foregoing reservations, experimental and theoretical treatments of hindered diffusion (Davidson and Deen, 1988a, 1988b; Maddox et al., 1992) allow a rough estimate of the plasmodesmal channel size available for cell-to-cell post-phloem movement in wheat grains. Assuming an absence of interaction

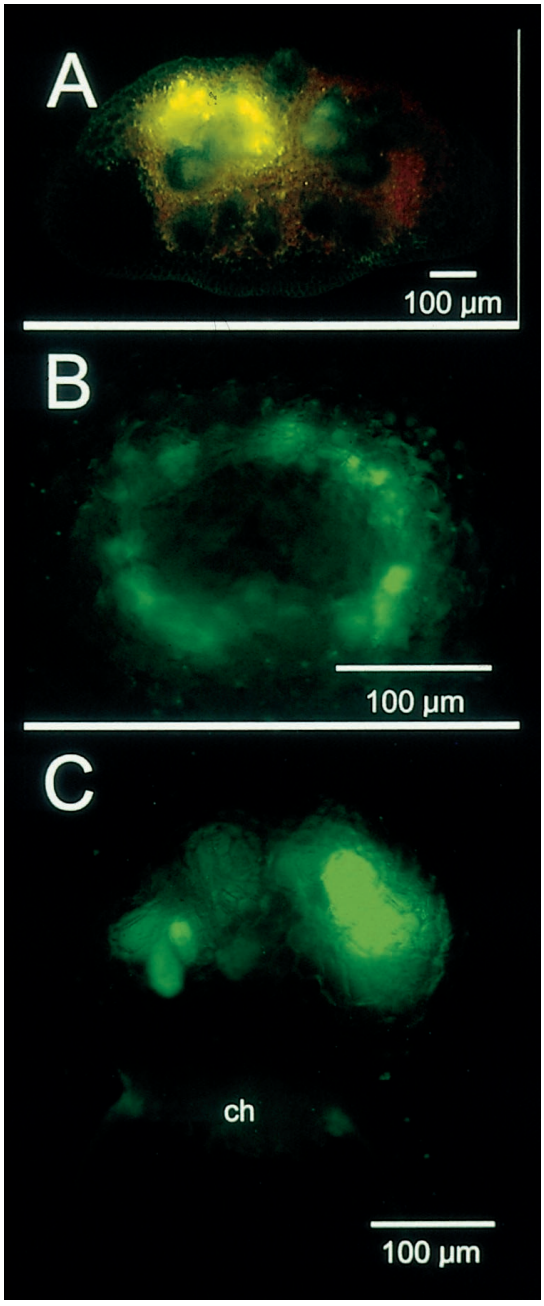

Figure 12. Distribution of F-dextrans after injection into rachilla sieve tubes. A, Considerable spreading to other vascular bundles occurred in the anastomosing connections immediately below the point of grain insertion on the rachilla (3-kD F-dextran). B, In the region of the xylem discontinuity in the pedicel, conducting sieve tubes surround the central core of modified tracheary elements (3-kD F-dextran). C, Unloading occurred from more sieve tubes compared with tracers injected into a grain sieve tube (70-kD F-dextran). ch, Chalaza.

between solute and pore and a R_s of 2.6 nm as the largest mobile tracer, these sources indicate that the channel would have to be about 1.5x this radius, or a diameter of approximately 8 nm, to allow appreciable mobility of such a large solute. This is about twice the channel diameter for plasmodesmata with an mass exclusion limit of 800 D (Terry and Robards, 1987; Fisher, 1999).

For reasons that are unclear (there was no evidence of sequestration of larger tracers into vacuoles), there was a tendency of some of the unloaded tracers to remain in cells immediately surrounding the phloem. Aside from this, the smaller tracers in particular appeared to diffuse evenly throughout the post-phloem pathway, moving at some points against the prevailing import of assimilates. Thus, cell-to-cell movement in these tissues appears to be dominated by diffusion (also, see Wang and Fisher, 1994b), although the tendency of the less-mobile 10- and 16-kD F-dextrans to accumulate in the nucellus (Fig. 7) suggests a minor transport contribution from bulk flow.

SE/CC Unloading

It has been suggested on the basis of tritiated water experiments (Jenner, 1985) that the sieve tubes may be discontinuous at the base of the grain (as are the xylem vessels; Zee and O'Brien, 1970). If so, proteins might be excluded there, leaving moot the question of their unloading in the grain. However, the movement of a variety of rachilla-injected tracers into the grain indicates that the sieve tubes are continuous, and there is no anatomical evidence that they are not (O'Brien et al., 1985).

In sharp contrast to movement along the post-phloem pathway, unloading of the SE/CC complex proceeds down a steep concentration and pressure differential between the complex and surrounding cells. In wheat grains, this differential is about 1.0 MPa (Fisher, 1995; Fisher and Cash-Clark, 2000), and in barley roots about 0.7 MPa (Pritchard, 1996) over a distance of only 0.5 μm (the length of the plasmodesmata). Thus, at this step, transport is primarily convective, in contrast to the predominance of diffusive transport in post-phloem movement (previous section).

Our finding that even the largest injected tracers could unload from the SE/CC complex, along with the consistent patchiness of their unloading, raises puzzling and presently unanswerable questions regarding the physical parameters of the unloading step. Quite large channels may be present in these plasmodesmata, or perhaps the unloading of larger tracers may occur as a result of structural damage to the plasmodesmata. Both of these possibilities will be addressed, since a definitive choice cannot presently be made.

If patchy unloading via large channels were in fact the pathway for solute movement out of the SE/CC complex, the apparent uniformity in the unloading of smaller solutes could result from their ready movement along the post-phloem pathway. This would obscure any initial small-scale unevenness, although it does not explain the frequently observed larger

scale difference in the unloading of large tracers along the length of the grain (e.g. at the distal third). However, failure to unload and the patchiness of unloading might result from plugging of plasmodesmata along stretches of the sieve tube without affecting unloading at other sites. Also, only a single sieve tube was injected, and there is no a priori reason to expect consistently uniform loading from each individual sieve tube.

Channels large enough to accommodate the movement of Ficoll molecules with an R_s of 11 nm would occupy much (perhaps all) of the 42-nm internal diameter reported for plasmodesmata present at this interface (Wang et al., 1995). While it is possible that shearing forces might distort their dimensions within the pores to a smaller physical radius, the highly cross-linked configuration and reported rigidity of Ficolls (Maddox et al., 1992, and refs. therein) indicate that such distortion would not be very pronounced. Also, judging from conformational effects on the movement of rigid solutes in small pores (Anderson, 1981), it seems unlikely that movement would be facilitated by distortion.

Pores sufficiently large enough to accommodate 400-kD Ficoll molecules would have a high hydraulic conductivity. Assuming, for example, that cylindrical pores 10 nm in radius and 0.5 μm long are present in these plasmodesmata, the volume rate of flow per pore with a 1-MPa pressure differential would be about 4×10^{-9} μL s^{-1}. Only about 3×10^4 such pores (approximately 10^3, for 21 nm pores) would be necessary to account for the total unloading rate of about 10 μL d^{-1} (Fisher, 1990). By comparison, Wang et al. (1995) report a total of 2.4×10^7 plasmodesmata at the juncture between the SE/CC complex and the surrounding parenchyma cells in wheat grains. With such a large pore size, only 0.1% of the plasmodesmata would be functioning at any given moment. It is also instructive to calculate the apparent pore size for unloading, assuming that all plasmodesmata are functional and that there are nine channels per plasmodesma (Terry and Robards, 1987). This yields a radius of about 1.1 nm, which is clearly too small. Thus, it is likely that some plasmodesmata at the SE/CC unloading interface are non-functional, or at least do not function all of the time.

If channels large enough to accommodate movement of the largest tracers are not normally present in plasmodesmata at the SE/CC unloading step, these tracers must have been unloaded as a result of damage to the plasmodesmata. Since the larger dextrans and proteins (e.g. GUS), in addition to Ficoll, appeared to cause similar "damage" (i.e. marked unevenness in unloading and, in co-injection experiments, apparent blockage of the smaller tracer from unloading over much of the sieve tube length), the mechanism appears similar in all cases. Plugging of the channels would seem to be the most likely common basis for the similar effects of such different molecules. If it occurred at a particular point in a channel, plugging might steepen the pressure gradient there and cause the plasmodesma to lose its structural integrity. Formation of such an abnormally large channel would presumably cause turgor in the adjoining parenchyma cell to increase, perhaps closing symplastic connections to contiguous parenchyma cells (Oparka and Prior, 1992). This would be consistent with the predominant coincidence of cell labeling when large and small tracers were co-injected. However, patchiness of unloading did not necessarily preclude subsequent post-phloem movement (e.g. GFP, 10- and 16-kD F-dextrans), perhaps because some plasmodesmata were not damaged or some recovery occurred. Also, patchy unloading of large tracers was just as consistent in detached grains, in which the turgor gradient across the SE/CC unloading pathway would presumably have been substantially less than in attached grains, arguing against a turgor-gradient-dependent damage mechanism.

Our observations leave open a wide range of possibilities for the dimensions of the channels involved in SE/CC unloading. Since even the largest tracer was unloaded, the upper limit is bounded only by the i.d. of the plasma membrane plasmodesmal sleeve, which is 42 nm (Wang et al., 1995). This seems the most appropriate estimate if the tracers did not damage plasmodesmal structure beyond simple blockage of some channels.

If the plasmodesmata were damaged, molecular size provides minimal information regarding undisturbed channel dimensions. However, to the extent that uniformity of unloading along the phloem might be taken to indicate an absence of interaction between the tracer and channel, molecules at least as large as the 3-kD F-dextran (R_s = 1.2 nm) appear to be almost completely unhindered. Judging from Davidson and Deen's (1988b) theoretical analysis of hindered convective movement of flexible molecules through small pores, this suggests a minimum pore diameter of approximately 4 nm. This is about the size of channels in plasmodesmata with a diffusional mass exclusion limit of 800 kD (Fisher, 1999). Even this conservatively small value is subject to the reservation, previously noted, that dextran movement through small pores has been observed in two systems to be enhanced, although the reasons for this are as yet unknown.

A Role for Plasmodesmal Recognition Factors in STEPs?

The possibility that even fairly small dextrans and proteins may cause plugging of plasmodesmata at the SE/CC unloading step suggests a possible role for plasmodesmal recognition factors in STEPs, implied by their ability to up-regulate the dextran mass exclusion limit in mesophyll cells (Balachandran et

al., 1997). Since these proteins range up to about 70 kD in wheat (Fisher et al., 1992), they too would seem capable of causing plasmodesmal plugging unless their passage were facilitated in some manner by specific interaction with the plasmodesmata. Also, since STEPs have been shown to up-regulate the plasmodesmal mass exclusion limit, their continued presence in the translocation stream may be a factor in the generally higher mass exclusion limits of plasmodesmata involved in post-phloem movement and, possibly, SE/CC unloading. Such plasmodesmal/STEP interaction would have to be specific, however, since unloading from the SE/CC complex is limited almost entirely to sinks. Also, within sinks, not all plasmodesmata are conductive (e.g. assimilates do not readily enter chlorenchyma cells bordering the vascular parenchyma in the wheat grain).

Cells of the Post-Phloem Pathway Apparently Function as an Important Detoxification Site

Because solute uptake and transport by plants is not entirely selective, plants have developed a number of approaches to neutralize potentially harmful foreign chemicals (xenobiotics). This includes various derivatization processes (Sandermann, 1992), with the products often being stored in vacuoles. As active centers of solute import, sink tissues appear to require a significant capacity for such detoxification, as has been noted for the import of fluorescent tracers into Arabidopsis root tips (Wright et al., 1996). Judging from the efficiency of vacuolar sequestration of several smaller tracers, including phloem-imported 3-kD R-dextran, the post-phloem pathway of wheat grains appears to be a particularly active site of sequestration. Although other processes might also be operative, the rapid sequestration of a strongly fluorescent product into the vacuole on exposure to BmCl strongly implicates the operation of the well-studied glutathione-dependent detoxification pathway (Coleman et al., 1997) in the vascular parenchyma.

MATERIALS AND METHODS

Plant Material

Wheat (*Triticum aestivum* L. cv SUN 9E) plants were grown in a growth chamber on a 16-h photoperiod at a photosynthetic photon flux density of 450 μmol m^{-2} s^{-1} at a day/night regime of 22°C/16°C. Plants were kept well watered and were irrigated with a complete nutrient solution once a week. Grain filling was complete about 30 DPA; plants were used at 15 to 22 DPA.

Aphids and Stylet Cutting

Aphids (*Rhopalosiphum padi* L.) were caged on the ear overnight and their stylets were cut by radio frequency microcautery the next morning (Fisher and Frame, 1984). Because injections were made at locations on the ear that are not normally accessible for feeding, those sites were exposed by removing the overlying structures. For feeding on the rachilla (the spikelet axis), this meant removing the glumes and distal-most grains of each spikelet to expose the rachilla just below the "c" (third from the bottom) grain of the spikelet. For feeding on the grains, where most injections were made, all but the basal ("a" or "b") grain of each spikelet was removed, as well as the palea of the remaining basal grain. This exposed the groove, or crease, of the grain, at the bottom of which lies the single vascular bundle supplying the grain.

Injections were also made into the phloem of detached grains. In this case, the stylets were cut as above and the grains were detached from the plant by breaking the grain pedicel. Moistened filter paper strips were draped over the detached grain during injection. Stylets continue to exude for several hours or longer, although at slow rates, on detached grains (Fisher and Gifford, 1986; Fisher, 1995).

Injection of Tracers into the Sieve Tube

The approach to the injection of solutes into the sieve tube was adapted from procedures used for manometric measurements of turgor pressure (Fisher and Cash-Clark, 2000). This involved gluing a length of capillary tubing, sealed at one end, to an exuding stylet and allowing the exudate to compress the air column in the manometer. When exudate flow ceases, turgor in the sieve tube is balanced by air pressure in the manometer; heating the end of the manometer raises the pressure above the balance point, forcing exudate back into the sieve tube. Compared with other methods, this approach has the advantage that the seal to the stylet is completely undisturbed by attachment to some pressure-generating device.

Manometers for injection experiments (Fig. 13) were modified to minimize exudate flow into the manometer, which would dilute the tracer solution to be injected. Most of the manometer length consisted of plastic-clad silica tubing, 150-μm o.d., 100-μm i.d. (Polymicro Technologies, Phoenix). A glass tip pulled from capillary tubing was

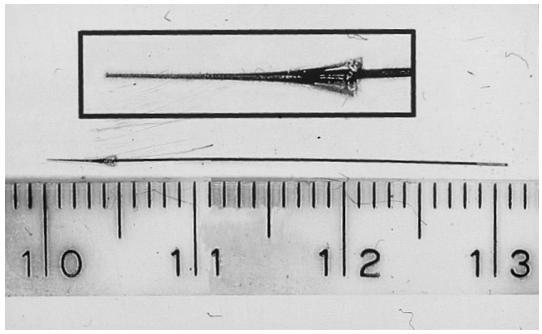

Figure 13. Configuration of an injection manometer, consisting of a 3-cm length of 100 μm i.d. plastic-clad silica tubing sealed into a glass tip (inset) to provide increased volume near the stylet. Before an injection, the manometer was filled with tracer solution. (Here, R-dextran was used for visibility). A 1- to 2-mm length was left unfilled at the distal end (right), which was sealed with a plug of quick-setting epoxy.

sealed to one end with cyanoacrylate adhesive to provide a reservoir. The smaller tip also facilitated sealing to stylets in the confines of the crease region. About 1 h before an experiment, the manometer was filled with tracer solution to within 1 to 2 mm of the end of the silica tubing, which was then sealed with quick-setting epoxy. Filled manometers were stored in a humid container.

After sealing an injection manometer to a stylet, heating of the manometer's free end was accomplished by slipping the end into a 2.5-cm length of 1-mm i.d. glass tubing mounted in a groove in an aluminum block, which was warmed by a resistance heater embedded in the block. The block, resistor, and most of the glass tubing were surrounded by insulation except for the upper surface of the tubing, 1 cm of which was left exposed to allow viewing of the manometer. Heating was controlled by a rheostat, and temperature was monitored by a thermocouple in the tubing. The manometer was advanced progressively into the heated tubing as the gas pocket expanded, forcing tracer solution from the manometer tip. Temperatures of about 200°C to 225°C were required for injection. (It should be noted that expansion of the gas pocket was driven by the vapor pressure of water, not by the expansion of air. Thus, although pressure could not be monitored directly, its approximate value could be determined from a standard table relating water vapor pressure to temperature.)

Tracers and Tracer Solutions

With one exception, fluorescent tracers were obtained from Molecular Probes (Eugene, OR). β-Glucuronidase (GUS) and 20-kD fluorescein-labeled dextran (F-dextran) were purchased from Sigma-Aldrich (St. Louis). GFP was purchased from CLONTECH Laboratories (Palo Alto, CA). F-Dextrans of narrowly defined sizes from a Stokes radius (R_s) of 2.0 nm (approximately 10 kD) to 2.6 nm (approximately 16 kD) were available from earlier work (Wang and Fisher, 1994b). Relationships between molecular size and molecular mass were interpolated from literature values (see "Discussion").

All tracers, including GFP and GUS, were used at a concentration of 1 mg mL^{-1} in wheat phloem exudate collected from exuding aphid stylets on a peduncle and made up to a concentration of 850 mOsm (Fisher et al., 1992). To remove low-M_r solutes present in the GFP and GUS solutions supplied by the manufacturers, a 100-μL aliquot of the sample was passed through a 3-mL column of Sephadex-G25 equilibrated with water. The first 0.5 mL after the void volume was collected on a silanized microscope slide, quickly taken to dryness under vacuum, and dissolved promptly in an appropriate volume of exudate. Stock solutions of tracers in phloem exudate were stored at −20°C.

Sectioning and Microscopy

Hand-cut fresh sections, 150 to 200 μm in thickness, were mounted in endosperm cavity perfusion medium (Wang and Fisher, 1994a; 14 mM 2-[N-morpholino]-ethanesulfonic acid [MES], 2 mM KPO_4, and 1.3 mM $MgCl_2$ made to 300 mOsm with mannitol and at pH 6.5). Tissue was sectioned in most cases soon after the 40- to 80-min injection period. For larger tracers of uncertain mobility, some grains were left on the plant after injection for 3 to 20 h before sectioning.

Sections were viewed by epifluorescence microscopy with a microscope (Ortholux II, Leitz, Midland, Ontario, Canada) fitted with a xenon light source and a digital camera (DKC-5000, Sony, Tokyo). In most cases, fluorescein conjugates and GFP were viewed with Omega filter XF23 (Omega Optical, Inc., Brattelboro, VT) which eliminated most autofluorescence. An H2 filter cube (Leitz), which has a long wavelength band-pass barrier filter, was used when tissue autofluorescence helped to identify anatomical features. Rhodamine conjugates were viewed with Omega filter XF34.

The procedures given by Jefferson et al. (1987) were followed for the histochemical localization of GUS activity.

Tracer Stability

Two approaches were used to verify that fluorescence presumed to be associated with macromolecules was not due to some degradation product. In one, nuclei were visualized with Hoechst stain (10 μg mL^{-1} for 20 min) to compare with the distribution of presumed F-dextran or fluorescein-labeled Ficoll (F-Ficoll) fluorescence. Also, fresh sections containing injected tracers were immersed for 5 min in boiling water and reexamined at later intervals to verify retention of larger tracers by the cell walls.

Received October 13, 1999; accepted December 21, 1999.

LITERATURE CITED

Anderson JL (1981) Configurational effect on the reflection coefficient for rigid solutes in capillary pores. J Theor Biol **90:** 405–426

Balachandran S, Xiang Y, Schobert C, Tompson GA, Lucas WJ (1997) Phloem sap proteins from *Cucurbita maxima* and *Ricinus communis* have the capacity to traffic cell to cell through plasmodesmata. Proc Natl Acad Sci USA **94:** 14150–14155

Bohrer MP, Patterson GD, Carrol PJ (1984) Hindered diffusion of dextran and ficoll in microporous membranes. Macromolecules **17:** 1170- 1173

Bret-Hart MS, Silk WK (1994) Nonvascular, symplasmic diffusion of sucrose cannot satisfy the carbon demands of growth in the primary root tip of *Zea mays* L. Plant Physiol **105:** 19–33

Coleman JOD, Randall R, Blake-Kalff MMA (1997) Detoxification of xenobiotics in plant cells by glutathione conjugation and vacuolar compartmentalization: a fluo-

rescent assay using monochlorobimane. Plant Cell Environ **20:** 449–460

Davidson MG, Deen WM (1988a) Hydrodynamic theory for the hindered transport of flexible macromolecules in porous membranes. J Membr Sci **35:** 167–192

Davidson MG, Deen WM (1988b) Hindered diffusion of water-soluble macromolecules in membranes. Macromolecules **21:** 3474–3481

Ding B (1998) Intercellular protein trafficking through plasmodesmata. Plant Mol Biol **38:** 279–310

Fisher DB (1990) Measurement of phloem transport rates by an indicator-dilution technique. Plant Physiol **94:** 455–462

Fisher DB (1995) Phloem unloading in developing wheat grains. *In* HG Pontis, GL Salerno, EJ Echeverria, eds, Sucrose Metabolism, Biochemistry, Physiology, and Molecular Biology. American Society of Plant Physiologists, Rockville, MD, pp 206–215

Fisher DB (1999) The estimated pore diameter for plasmodesmal channels in the *Abutilon* nectary trichome should be about 4 nm, rather than 3 nm. Planta **208:** 299–300

Fisher DB, Cash-Clark CE (2000) Gradients in water potential and turgor pressure along the translocation pathway during grain filling in normally watered and water-stressed wheat plants. Plant Physiol **123:** 139–147

Fisher DB, Frame JM (1984) A guide to the use of the exuding stylet technique in phloem physiology. Planta **161:** 385–393

Fisher DB, Gifford RM (1986) Accumulation and conversion of sugars by developing wheat grains: VI. Gradients along the transport pathway from the peduncle to the endosperm cavity during grain filling. Plant Physiol **82:** 1024–1030

Fisher DB, Oparka KJ (1996) Post-phloem transport: principles and problems. J Exp Bot **47:** 1141–1154

Fisher DB, Wu Y, Ku MSB (1992) Turnover of soluble proteins in the wheat sieve tube. Plant Physiol **100:** 1433–1441

Imlau A, Truernit E, Sauer N (1999) Cell-to-cell and long-distance trafficking of the green fluorescent protein in the phloem and symplastic unloading of the protein into sink tissues. Plant Cell **11:** 309–322

Jefferson RA, Kavanagh TA, Bevan MW (1987) GUS fusions: β-glucuronidase as a sensitive and versatile gene fusion marker in higher plants. EMBO J **6:** 3901–3907

Jenner CF (1985) Transport of tritiated water and ^{14}C-labelled assimilate into grains of wheat: III. Diffusion of THO through the stalk. Aust J Plant Physiol **12:** 595–608

Johnson EM, Berk DA, Jain RK, Deen WM (1996) Hindered diffusion in agarose gels: test of effective medium model. Biophys J **70:** 1017–1026

Jorgensen KE, Moller JV (1979) Use of flexible polymers as probes of glomerular pore size. Am J Physiol **236:** F103–F111

Laurent TC, Granath KA (1967) Fractionation of dextran and Ficoll by chromatography on Sephadex G-200. Biochim Biophys Acta **136:** 191–198

le Maire M, Aggerbeck LP, Monteilhet C, Andersen JP, Moller JV (1986) The use of high-performance liquid chromatography for the determination of size and molecular weight of proteins: a caution and a list of membrane proteins suitable as standards. Anal Biochem **154:** 525–535

Maddox DA, Deen WM, Brenner BM (1992) Glomerular filtration. *In* EE Windhager, ed, Handbook of Physiology, Renal Physiology, Section 8, Vol 1. American Physiological Society, Bethesda, MD, pp 545–638

Mezitt LA, Lucas WJ (1996) Plasmodesmal cell-to-cell transport of proteins and nucleic acids. Plant Mol Biol **32:** 251–273

Nakamura S, Hayashi H, Mori S, Chino M (1993) Protein phosphorylation in the sieve tubes of rice plants. Plant Cell Physiol **34:** 927–933

O'Brien TP, Sammut ME, Lee JW, Smart MG (1985) The vascular system of the wheat spikelet. Aust J Plant Physiol **12:** 487–512

Oparka KJ, Prior DAM (1992) Direct evidence for pressure-generated closure of plasmodesmata. Plant J **5:** 741–750

Oparka KJ, Roberts AG, Boevink P, Santa Cruz S, Roberts IM, Pradel KS, Imlau A, Kotlizky G, Sauer N, Epel B (1999) Simple, but not branched, plasmodesmata allow the nonspecific trafficking of proteins in developing tobacco leaves. Cell **97:** 743–754

Ormo M, Cubitt AB, Kallio K, Gross LA, Tsien RY, Remington SJ (1996) Crystal structure of the *Aequorea victoria* green fluorescent protein. Science **273:** 1392–1395

Patrick JW (1997) Phloem unloading: sieve element unloading and post-sieve element transport. Annu Rev Plant Physiol Mol Biol **48:** 191–222

Pritchard J (1996) Aphid stylectomy reveals an osmotic step between sieve tube and cortical cells in barley roots. J Exp Bot **47:** 1519–1524

Rennke HG, Venkatachalam MA (1979) Glomerular permeability to macromolecules: effect of molecular configuration on the fractional clearance of uncharged dextran and neutral horseradish peroxidase in the rat. J Clin Invest **63:** 713–719

Sandermann H (1992) Plant metabolism of xenobiotics. TIBS **17:** 82–84

Shi Y, Wang MB, Powell KS, van Damme E, Hilder VA, Gatehouse AMR, Boulter D, Gatehouse JA (1994) Use of the rice sucrose synthase-1 promoter to direct phloem-specific expression of β-glucuronidase and snowdrop lectin genes in transgenic tobacco plants. J Exp Bot **45:** 623–631

Terry BR, Robards AW (1987) Hydrodynamic radius alone governs the mobility of molecules through plasmodesmata. Planta **171:** 145–157

Wang HL, Offler CE, Patrick JW (1995) The cellular pathway of photosynthate transfer in the developing wheat grain: II. A structural analysis and histochemical studies of the pathway from the crease phloem to the endosperm cavity. Plant Cell Environ **18:** 373–388

Wang N, Fisher DB (1994a) Monitoring phloem unloading

and post-phloem transport by microperfusion of developing wheat grains. Plant Physiol **104:** 7–16

Wang N, Fisher DB (1994b) The use of fluorescent tracers to characterize the post-phloem transport pathway in maternal tissues of developing wheat grains. Plant Physiol **104:** 17–27

Wright JP, Fisher DB (1980) Direct measurement of sieve tube turgor pressure using severed aphid stylets. Plant Physiol **65:** 1133–1135

Wright KM, Horobin RW, Oparka KJ (1996) Phloem mobility of fluorescent xenobiotics in *Arabidopsis* in relation to their physicochemical properties. J Exp Bot **47:** 1779–1787

Yang F, Moss LG, Phillips GN (1996) The molecular structure of green fluorescent protein. Nat Biotechnol **14:** 1246–1251

Zee SY, O'Brien TP (1970) A special type of tracheary element associated with "xylem discontinuity" in the floral axis of wheat. Aust J Biol Sci **23:** 783–781